

The Influence of Synthesis Parameters on FeO(OH) / Fe₂O₃ Formation by Hydrothermal Techniques

Madalina Popescu^a, Roxana Piticescu^a, Eugeniu Vasile^b, Dragos Taloi^{a,c},
Mirela Petriceanu^a, Maria Stoiciu^a, and Viorel Badilita^a

^a National R& D Institute for Non-Ferrous and Rare Metals – IMNR, Pantelimon, Ilfov, Romania

^b METAV CD, Bucharest, Romania

^c University “Politehnica” Bucharest, Faculty of Materials Science, Bucharest, Romania

Reprint requests to Roxana Piticescu. E-mail: roxana@imnr.ro

Z. Naturforsch. **2010**, 65b, 1024 – 1032; received March 8, 2010

In this paper, a hydrothermal method of high-pressure and low-temperature synthesis conditions is presented as a simple single-step technique to obtain crystalline nanoparticles of iron oxides. The aim of this work has been to demonstrate the influence of the main synthesis parameters on the formation of nanosized Fe₂O₃ particles using statistical methods and to establish the most significant effects. Based on mathematical pre-modeling calculations, the best reaction conditions for the hydrothermal process have been chosen, and controlled crystalline nanostructures of iron oxides could be prepared.

Key words: Fe₂O₃, High Pressure, Hydrothermal Synthesis, Correlation Analysis

Introduction

Oxides of iron are widely available in different forms such as α -Fe₂O₃, which occurs naturally as the mineral hematite, β -Fe₂O₃, γ -Fe₂O₃, occurring naturally as the mineral maghemite, ϵ -Fe₂O₃, FeO, α -FeOOH, and γ -FeOOH. Recently, nanosized iron oxides in their various forms have been investigated extensively for their magnetic, electronic, optical and electrochemical properties which make them suitable for a broad range of applications such as telecommunication, computer systems, photo-electrochemical solar cells, alkaline batteries, ferro-fluids, magneto-caloric refrigeration, biotechnology, environmental remediation, magnetic recording, and *in vivo* biomedicine [1,2]. Iron oxides are relatively inert, biocompatible and biodegradable, exhibit neither acute nor chronic toxicity, and are present in several living organisms, which makes them important for biomedical applications, like magnetically controlled drug delivery, use as contrast agents in magnetic resonance imaging, tissue repair, immunoassay, and detoxification of biological fluids [1,3].

There has been much interest in the development of synthetic methods to produce high-quality iron oxide samples. The traditional approach to iron oxide colloids has relied on the aqueous precipitation or hydrolysis of Fe²⁺ and/or Fe³⁺ salts, using different proto-

cols, namely slow hydrolysis, forced hydrolysis at high temperature, acidic hydrolysis at high temperature and hydrolysis in the presence of various additives [1,4]. A major drawback of these methods is that these materials can be poorly crystalline and polydisperse in many cases.

Recently, Y. Thomas He and co-workers [5] synthesized α -Fe₂O₃ nanoparticles by the forced hydrolysis of FeCl₃ at 98 °C, and H. Kitaura *et al.* prepared fine α -Fe₂O₃ nanoparticles by a mechanochemical and a solution process [6]. X. Liang *et al.* obtained maghemite microspheres (γ -Fe₂O₃) by the solvothermal method and a subsequent calcining process [7]. In 2002, V. Hiremath and A. Venkataraman prepared γ -Fe₂O₃ by a combustion method, showing that chemical homogeneity, fine grain structure, particle size and shape of ferrite affect the dielectrical properties, the electrical conductivity and the infrared spectra. The presence of α -impurities also contributes towards changes in these properties. Iron oxide (α -Fe₂O₃) was also synthesized by a microwave hydrothermal method which is known for its fast reaction kinetics. Spherical particles were formed with a high agglomeration degree [8,9]. A series of α -Fe₂O₃/FeOOH nanostructures with different morphologies, including spherical, cubic, chained sphere, and dendritic nanoparticles were synthesized at 140 °C by a novel hydrothermal method. The morphology and phase of α -Fe₂O₃/

FeOOH were controlled by adjusting the reaction time [10]. Unusual polyhedral structures of cubic Fe₃O₄ were fabricated in high yield *via* a facile hydrothermal method in the presence of the surfactant Cetyl trimethylammonium bromide (CTAB). The surfactant concentration determines the shape of the particles (hexagonal, dodecahedral, truncated octahedral, and octahedral) [11]. However, it is still a challenge to develop simple and reliable methods for the synthesis of iron oxide nanoparticles for use in biomedical applications.

In the present work, the hydrothermal method in high-pressure and low-temperature synthesis conditions has been used as a simple single-step technique to obtain crystalline nanoparticles of iron oxides. This method is well known for its advantages. Reaction takes place in an aqueous medium, without organic solvents or elimination of toxic vapors, making this method environmentally friendly. It has also reduced energy consumption. The aim of this work has been the investigation of the influence of the main synthesis parameters on the formation of nanosized Fe₂O₃ particles formation using statistical methods and to establish the most significant parameters. Based on mathematical calculations, the best reaction conditions for the hydrothermal process can be chosen, and crystalline nanostructures of iron oxides can be prepared in a controlled way.

Materials and Methods

Synthesis of iron oxide

Iron oxide was synthesized by the hydrothermal method under high-pressure conditions starting from commercial FeCl₃ powder (analytical grade) purchased from Merck and aqueous ammonia solution (25 % w/w) used without further purification. The reagents were mixed in distilled water at room temperature and stirred continuously. This precursor suspension was placed in a 300 mL stainless steel autoclave for the hydrothermal reaction. After the reaction was completed, the resulting suspension was filtered and the precipitate washed several times with distilled water and dried in an oven in air at 100 °C.

Characterization

The powders resulting from the hydrothermal syntheses were characterized with regard to their composition, structure and morphology. The chemical composition was determined by quantitative analysis. Struc-

Experimental points	Process parameters		
	x_1	x_2	x_3
1	-1	-1	-1
2	+1	-1	+1
3	+1	+1	-1
4	-1	+1	-1
5	+1	+1	+1
6	-1	+1	+1
7	+1	-1	-1
8	-1	-1	+1

Table 1. Matrix of experiments^a.

^a $x_i = \frac{z_i - z_i^0}{\Delta z_i}$, $i = 1-3$; $z_1^0 = 150$; $\Delta z_1 = 50$; $z_2^0 = 2.5$; $\Delta z_2 = 0.5$; $z_3^0 = 15$; $\Delta z_3 = 5$.

tural characterization was performed on a Bruker D8 Advance diffractometer in Bragg-Brentano diffraction geometry using CuK α radiation and the Diffrac^{plus} XRD Commender software (Bruker AXS). The microstructure and morphology of the samples were examined by electron microscopy using a Tecnai G2 F30 S-Twin Field Emission High Resolution Transmission Electron Microscope (HRTEM), with a 50–300 kV electron source and magnifications of 58 x – 970 kx (TEM) and 150 x – 230 Mx (STEM). The particle size of the iron oxide powders was measured using a Malvern ZetaSizer Nano ZS90 analysis system. Differential scanning calorimetry (DSC) analysis was carried out on a Netzsch DSC 200 F3 Maia calorimeter at a heating rate of 10 °C min⁻¹ from -20 °C to 600 °C in an Ar atmosphere.

Mathematical pre-modeling

Synthesis parameters, namely temperature (z_1), time (z_2) and pressure (z_3) were varied according to a complete factorial experiment (CFE), to establish their influence on the hydrothermal process and to take them into account as parameters for the mathematical modeling of the process. The complete factorial experiment assumes that each parameter is varied at two levels: maximum (+) and minimum (-). The combinations of all factors with these levels is the total number of experimental points which is $N = 2^3$ for this case. Starting from initial values of temperature (z_1^0), time (z_2^0) and pressure (z_3^0) and their range of variation between minimum and maximum level (Δz_i , $i = 1-3$), then the following matrix for the experiments is obtained (Table 1).

Results and Discussion

Chemical composition

Iron oxide powders prepared by the hydrothermal method have been characterized by chemical quantita-

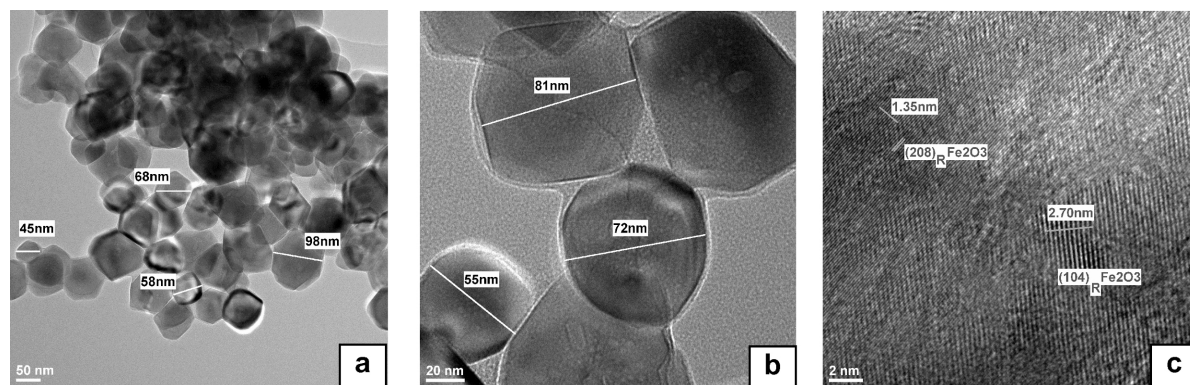


Fig. 3. TEM/HRTEM images of a representative sample synthesized at 200 °C/3 h/10 atm.

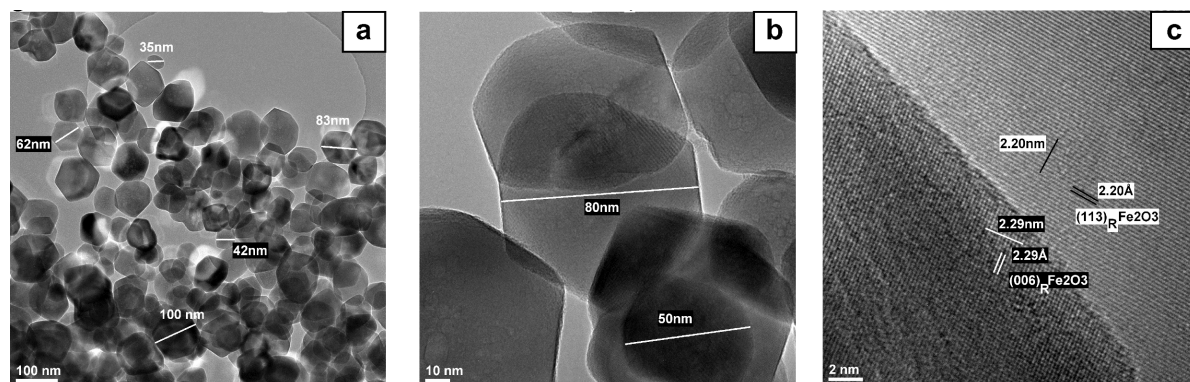


Fig. 4. TEM/HRTEM images of a representative sample synthesized at 200 °C/3 h/20 atm.

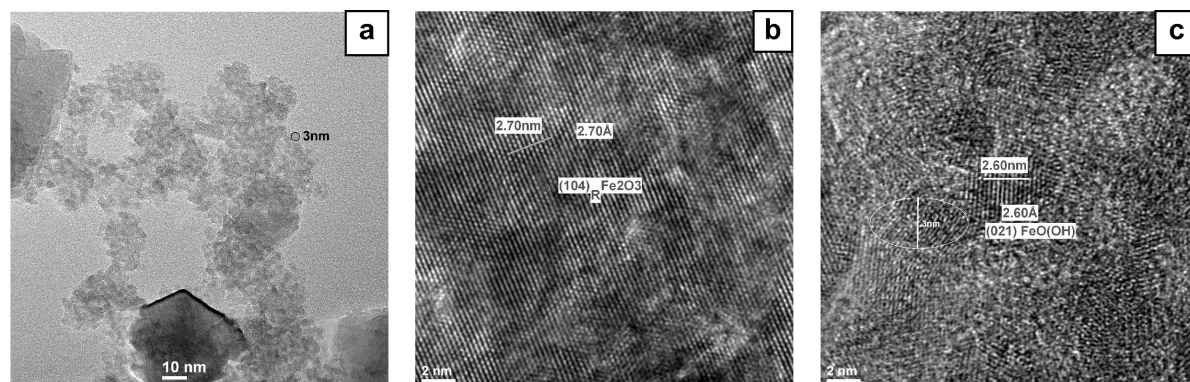


Fig. 5. a) TEM/HRTEM images of a representative sample synthesized at 100 °C/2 h/20 atm; b) HRTEM on large nanocrystallites, and (c) HRTEM on small nanocrystallites.

hexagonal crystalline platelets of about 45–90 nm in size. Internal micro- and mesoporosity (pore diameter < 10 nm) can be observed for these platelets. The possible presence of secondary phases such as goethite is suggested by the protecting film surrounding the Fe₂O₃ particles (Fig. 3b). Fig. 3c highlights the exist-

tence of two crystalline plane families: (208) rhombohedral Fe₂O₃ nanocrystallites and (104) rhombohedral Fe₂O₃ nanocrystallites. Also, inside the nanocrystalline particles one can see nanocrystallite limits and interfaces between nanocrystallites of the same particle.

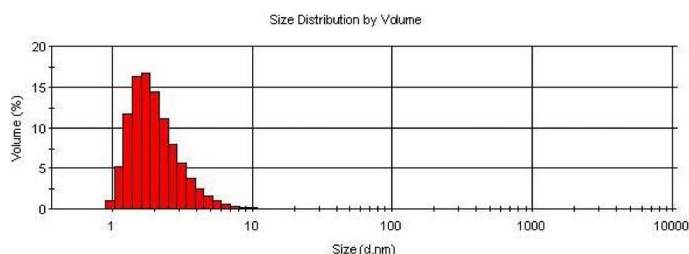


Fig. 6. Particle size distribution for a representative sample synthesized at 200 °C / 3 h / 10 atm.

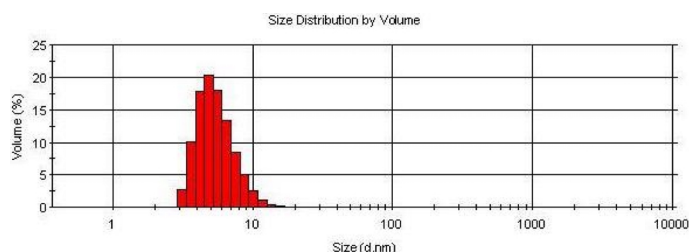


Fig. 7. Particle size distribution for a representative sample synthesized at 200 °C / 3 h / 20 atm.

In Fig. 4 one can observe crystalline polyhedral particles, with particle sizes below 100 nm (40–80 nm) and an internal porosity possibly due to dehydration and the appearance of holes (Fig. 4b). A HRTEM image of a sample synthesized at 200 °C / 3 h / 20 atm shows the presence of nanocrystalline iron oxide particles with (006) Fe₂O₃ and (113) Fe₂O₃. The image was taken at an interface between two particles.

Unlike the samples prepared at 200 °C / 3 h, in the case of the sample obtained at 100 °C / 2 h / 20 atm one observes both the presence of small, plate-like particles in the nanometer range (Fig. 5a) and large crystalline aggregates. Two phases are present as X-ray diffraction analysis has shown: (104) Fe₂O₃ and (021) FeO(OH) (Figs. 5b and c). It can be supposed that small iron oxide crystallites start forming but the final structure is disordered, almost amorphous (Fig. 5a). Small nanocrystallites (size about 3 nm) are ordered only for short distances. The crystallization process is not complete. The sample synthesized during 2 h at 100 °C consists of several phases of iron oxides. Fig. 5b demonstrates the presence of small Fe₂O₃ nanocrystalline particles.

Particle size measurements

Particle sizes for iron oxide powders were measured using a Malvern Zetasizer Nano ZS90 instrument. The Fe₂O₃ powders were stabilized as colloidal suspensions in water-ethanol solution, in the presence of the polyelectrolytic dispersant PAAS (sodium salt of poly-

Table 2. Average particle size of iron oxide.

No	Sample	<i>T</i> (°C)	<i>t</i> (h)	<i>P</i> (atm)	Average size (nm)	Size distribution
1	Fe9	100	2	10	36.6	bimodal
2	Fe8	100	2	20	18	bimodal
3	Fe4	100	3	10	27.5	monomodal
4	Fe6	100	3	20	19.3	monomodal
5	Fe7	200	2	10	6.1	monomodal
6	Fe2	200	2	20	5.3	monomodal
7	Fe3	200	3	10	3.8	monomodal
8	Fe5	200	3	20	7.2	monomodal

acrylic acid). The obtained values are summarized in Table 2.

Particle size distributions for some representative samples are presented in Figs. 6 and 7. The average particle size decreases with increasing temperature, time and pressure.

DSC studies

Results obtained from thermal analyses are summarized in Table 3. Some representative DSC curves are depicted in Fig. 8.

As one can see in Fig. 8, hydrothermally prepared Fe₂O₃ seems to be a mixture of iron hydroxides: α-FeO(OH) (goethite), α-FeO(OH)·*n*H₂O (limonite) and γ-FeO(OH) (lepidocrocite). Based on these findings, one can propose two reaction steps for Fe₂O₃ formation under hydrothermal conditions:

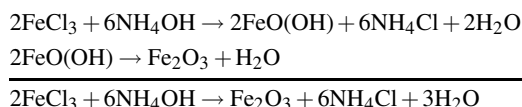


Table 3. DSC data (specific heat, transformation enthalpy and thermal effect).

Sample	Synthesis conditions			DSC data				Possible assignment of DSC peak
	<i>T</i> (°C)	<i>t</i> (h)	<i>P</i> (atm)	<i>C_p</i> (kcal mol ⁻¹ K ⁻¹)	ΔH (kcal mol ⁻¹)	Peak (°C)	Thermal effect	
Fe9	100	2	10	0.17	7.9	109.1	endothermic	water elimination
				0.04	0.22	313	endothermic	OH groups elimination from goethite, α -FeO(OH)
				0.014	-2.68	458	exothermic	polymorphic transformation γ -Fe ₂ O ₃ - α -Fe ₂ O ₃
Fe8	100	2	20	0.11	4.85	100.6	endothermic	water elimination
				0.05	0.57	316	endothermic	OH groups elimination from goethite, α -FeO(OH)
				0.019	0.141	433.4	endothermic	OH groups elimination from limonite, α -FeO(OH)· <i>n</i> H ₂ O
Fe4	100	3	10	0.07	-	93.4	endothermic	water elimination
				0.03	-	299.5	weakly endothermic	OH groups elimination from goethite, α -FeO(OH)
				0.026	-	399	very weakly endothermic	OH groups elimination from limonite, α -FeO(OH)· <i>n</i> H ₂ O
Fe6	100	3	20	0.07	2.61	93.9	endothermic	water elimination
				0.069	0.94	323.2	endothermic	OH groups elimination from goethite, α -FeO(OH)
Fe7	200	2	10	0.034	-	84.7	endothermic	water elimination
				0.034	-	304.4	endothermic	OH groups elimination from goethite, α -FeO(OH)
				0.031	-	87.9	endothermic	water elimination
Fe2	200	2	20	0.03	-	282.2	endothermic	OH groups elimination from goethite, α -FeO(OH)
				0.028	-	344	very weakly endothermic	OH groups elimination from goethite, α -FeO(OH)
				0.03	-	401.2	weakly endothermic	OH groups elimination from limonite, α -FeO(OH)· <i>n</i> H ₂ O
Fe3	200	3	10	0.029	-	90.6	endothermic	water elimination
				0.029	-	275.1	endothermic	OH groups elimination from goethite, α -FeO(OH)
				0.031	-	393.2	endothermic	OH groups elimination from limonite, α -FeO(OH)· <i>n</i> H ₂ O
Fe5	200	3	20	0.032	0.083	81.9	endothermic	water elimination
				0.032	0.09	288.5	endothermic	OH groups elimination from goethite, α -FeO(OH)

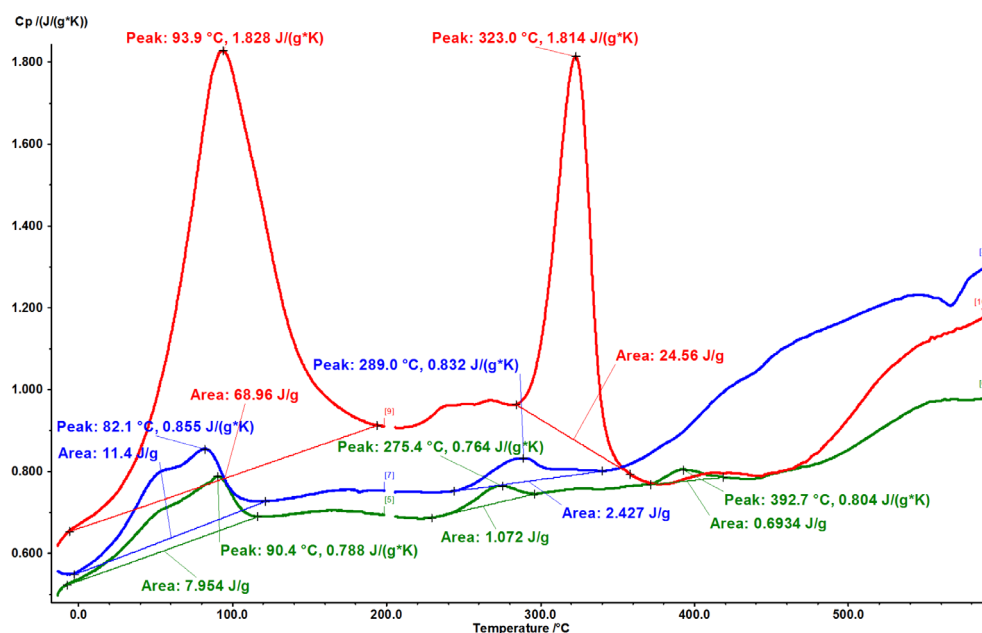


Fig. 8. Some representative DSC curves.

The endothermic effect arising between 250 and 360 °C can be explained by dehydration of goethite and formation of hematite (α -Fe₂O₃), while the effect

at around 350–400 °C is probably due to limonite dehydration [12]. Impurities can lead to small shifts of the transformation temperature (see Fig. 8).

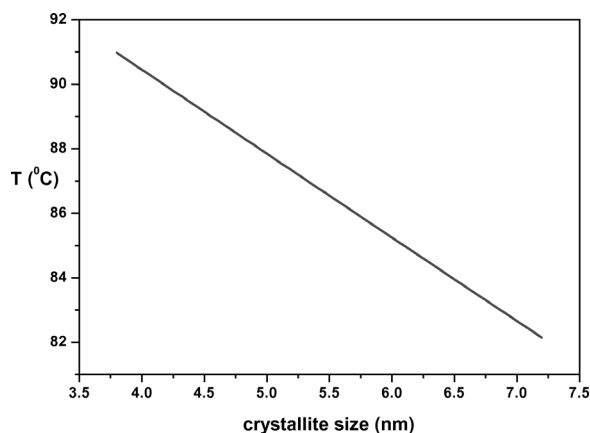


Fig. 9. Peak of water elimination *versus* crystallite size.

The theoretical composition of goethite is 89.9% Fe₂O₃ and 10.1% H₂O. If the water content is higher than that, as indicated by the chemical formula, the mineral is named limonite [12]. Goethite-limonite minerals show only one thermal effect in the DSC curves, accompanied by a mass loss as a consequence of water elimination and ferric oxide being formed as hematite.

It is supposed that 2 h of synthesis time for ferric oxide prepared by the hydrothermal method favor the formation of a higher amount of limonite (α -FeO(OH)·*n*H₂O), while 3 h of synthesis lead to goethite as the major iron oxide phase. Also, in the case of powders prepared at 200 °C, all three forms of iron hydroxyde – goethite, limonite and lepidocrocite – were observed, probably in equal proportions. Thermal effects that appear as a consequence of all these phase transformations are small.

The evolution of the DSC peak assigned to water elimination as a function of the average crystallite size is presented in Fig. 9, where *T* represents the temperature corresponding to a DSC peak. One can see that temperature values corresponding to water elimination in the DSC curve decrease with increasing crystallite size. Based on the fact that oxides with smaller crystallite size have a higher specific surface and a higher reactivity, we can assume that samples with larger particle size are not entirely crystalline and act as amorphous materials, whereas samples with lower particle size are more stable and nanocrystalline.

Mathematical pre-modeling

Mathematical pre-modeling of the hydrothermal synthesis of iron oxide was carried out using corre-

Experimental points	Process parameters			Process performance	Table 4. New matrix of experiments.
	<i>x</i> ₁	<i>x</i> ₂	<i>x</i> ₃	<i>y</i>	
1	-1	-1	-1	36.58	
2	+1	-1	+1	17.98	
3	+1	+1	-1	27.54	
4	-1	+1	-1	19.29	
5	+1	+1	+1	6.094	
6	-1	+1	+1	5.269	
7	+1	-1	-1	3.872	
8	-1	-1	+1	7.213	

lation analysis which is a statistical method that estimates the connections between different factors influencing the process and its performance. In our case, the particle size was selected as an indicator of the process performance. The matrix of experiments after the particle size measurements using a Malvern Zetasizer Nano SZ90 system is presented in Table 4.

Significant factors among parameters that influence the hydrothermal process (temperature, time and pressure) and significant interactions between factors are selected based on statistical criteria and further used as process parameters for the mathematical model.

Three types of correlation analysis were used for this purpose: simple correlation analysis, partial correlation analysis and multiple correlation analysis.

Simple correlation analysis

In this case the influence of each factor on the hydrothermal process is calculated taking also into account the interactions between both factors. In order to establish a correlation between the two factors, a simple correlation coefficient r_{xy} is calculated using [13]

$$r_{xy} = \frac{\sum_{i=1}^n x_i y_i - n \bar{x} \bar{y}}{(n-1) s_x s_y} \quad (1)$$

with

$$s_x = \sqrt{\frac{1}{n-1} \sum_{i=1}^n (x_i - \bar{x})^2} \quad s_y = \sqrt{\frac{1}{n-1} \sum_{i=1}^n (y_i - \bar{y})^2}$$

where s_x , s_y represent the mean square deviations and $\bar{x} = (1/n) \sum_{i=1}^n x_i$ and $\bar{y} = (1/n) \sum_{i=1}^n y_i$.

The simple correlation coefficient r varies between -1 and 1 ($-1 \leq r \leq 1$). $r = 0$ indicates that no correlation exists between the respective two factors.

In our case, simple correlation coefficients r_{xy} were calculated using the MATHCAD 14.0 software, and the following values were obtained: $r_{x_1 y} = -0.88$; $r_{x_2 y} = -0.089$; $r_{x_3 y} = -0.271$.

Significance testing of simple correlation coefficients was made using [13]

$$t_{x_i y} = |r_{x_i y}| \sqrt{\frac{n-2}{1-R_{x_i y}}} \text{ for } i = 1, 2, 3, \quad (2)$$

where $R_{x_i y} = r_{x_i y}^2$ represents the determination coefficient, $t_T = t_{0.05} = 2.447$ is a tabled value, and

$$t_{x_1 y} > t_T = 1; \quad t_{x_2 y} > t_T = 0; \quad t_{x_3 y} > t_T = 0.$$

These inequalities show that there is a simple correlation between the variable x_1 (temperature) and the process performance y (particle size).

Partial correlation analysis

In this case the influence of each factor on the hydrothermal process is calculated separately, and the other two factors are considered to be negligible. In order to establish a correlation between the two factors, the partial correlation coefficient $r_{yx_{i-1}x_1x_2\dots x_k}$ is calculated using [13]

$$r_{yx_{i-1}x_1x_2\dots x_k} = -P_{1i}/\sqrt{P_{11}P_{ii}} \text{ for } i > 1, \quad (3)$$

where P_{11} , P_{1i} and P_{ii} represent algebraic complements of the correlation determinant P reported for the elements r_{yy} , $r_{yx_{i-1}}$, $r_{x_{i-1}x_{i-1}}$:

$$P = \begin{pmatrix} 1 & r_{x_1 y} & r_{x_2 y} & r_{x_3 y} \\ r_{x_1 y} & 1 & r_{x_1 x_2} & r_{x_1 x_3} \\ r_{x_2 y} & r_{x_1 x_2} & 1 & r_{x_2 x_3} \\ r_{x_3 y} & r_{x_1 x_3} & r_{x_2 x_3} & 1 \end{pmatrix}. \quad (4)$$

In our case, partial correlation coefficients were calculated using the MATHCAD 14.0 software giving the values

$$r_{x_1 y \cdot x_2 x_3} = -0.918; \quad r_{x_2 y \cdot x_1 x_3} = -0.228; \\ r_{x_3 y \cdot x_1 x_2} = -0.58.$$

Significance testing of partial correlation coefficients was made using [13]

$$t_{x_i y \cdot x_j x_k} = |r_{x_i y \cdot x_j x_k}| \sqrt{\frac{n-2-e}{1-r_{x_i y \cdot x_j x_k}^2}} \quad (5)$$

where $n-2-e$ represents the number of degrees of freedom, e is the number of independent variables excluded ($e = 2$), $t_T = 2.201$ is a tabled value, and

$$t_{x_1 y \cdot x_2 x_3} = 4.622; \quad t_{x_2 y \cdot x_1 x_3} = 0.469; \\ t_{x_3 y \cdot x_1 x_2} = 1.425.$$

It can be observed that only $t_{x_1 y \cdot x_2 x_3} > t_T$ so that there is also a partial correlation between the x_1 variable (temperature) and the process performance y (particle size). This confirms the results obtained from the simple correlation analysis.

Multiple correlation analysis

This analysis shows the correlation between the performance of the process (particle size) and the three factors (temperature, time, pressure) that influence the process. The multiple correlation coefficient $r_{yx_1x_2x_3}$ expresses the degree of linear dependence between y (particle size) and the group of variables x_1, x_2, x_3 . It is calculated using [13]

$$r_{y \cdot x_1 x_2 x_3} = \sqrt{1 - P/P_{11}}, \quad (6)$$

where $0 \leq r_{y \cdot x_1 x_2 x_3} \leq 1$ and P is the correlation determinant as defined in Eq. 4.

If $r_{y \cdot x_1 x_2 x_3} = 1$, it can be considered that there is a functional connection between y and x_1, x_2, x_3 . If $r_{y \cdot x_1 x_2 x_3} = 0$ it can be considered that y is not dependent of x_1, x_2, x_3 .

In our case, the multiple correlation coefficient $r_{y \cdot x_1 x_2 x_3}$ was calculated using the MATHCAD 14.0 software resulting in $r_{y \cdot x_1 x_2 x_3} = 0.925$.

Significance testing of multiple correlation coefficients was made using the Fisher criterion. The calculated value is $F_C = 7.871$, and the tabled value is $F_T = 6.591$. With $F_C > F_T$ there is a multiple correlation between the performance of the process (particle size) and the three factors (temperature, time, pressure) that influence the process.

Conclusion

Based on experiments planned to obtain ferric oxide, it was found that samples synthesized at 200 °C/3 h are crystalline, have the lowest polydispersity, are characterized by crystalline planes and represent a mixture of Fe₂O₃ iron oxide (hematite) and FeO(OH) iron oxide hydroxides (α and γ). Particle sizes are below 90 nm, and small crystallite sizes of about 4–6 nm are present according to HRTEM and Malvern Zetasizer measurements. Samples synthesized at 100 °C present agglomerations and are made of two phases, hematite and goethite. Iron oxide nanoparticles predominate in the case of powders synthesized at 200 °C. Although the pressure does not seem to be a

significant factor for the performance of the hydrothermal process, an increase of pressure leads to smaller average particle size and higher reaction yield in the Fe₂O₃ synthesis. Based on these results and according to correlation analysis, optimized synthesis parameters for Fe₂O₃ nanopowders with potential medical applications were established.

Acknowledgements

We are grateful to the National Fond Nucleu Programme PN 09 24 02 03/2009 for financial support and to Dr. F. Stoiu for fruitful discussions regarding phase transformations and structural characterization.

-
- [1] A. Kumar, A. Singhal, *Nanotechnology* **2007**, *18*, 475703 (7pp).
- [2] Y. J. Park, K. M. Sobahan, C. K. Hwangbo, *Surface & Coatings Technology* **2009**, *203*, 2646.
- [3] K. J. Landmark, Dissertation, University of Michigan, **2008**, p. 57.
- [4] W. W. Yu, J. C. Falkner, C. T. Yavuz, V. L. Colvin, *Chem. Commun.* **2004**, 2306–2307.
- [5] Y. Thomas He, J. Wan, T. Tokunaga, *J. Nanopart. Res.* **2008**, *10*, 321–332.
- [6] H. Kitaura, K. Takahashi, F. Mizuno, A. Hayashi, K. Tadanaga, M. Tatsumisago, *Power Sources* **2008**, *183*, 418–421.
- [7] X. Liang, B. Xi, S. Xiong, Y. Zhu, F. Xue, Y. Qian, *Mater. Res. Bull.* **2009**, *44*, 2233–2239.
- [8] V. Hiremath, A. Venkataraman, *Bull. Mater. Sci.* **2003**, *26*, 391–396.
- [9] A. S. Brito, J. Maul, A. L. M. Oliveira, S. J. G. Lima, A. G. Souza, I. Garcia, D. Keyson, ICAM, *11th International Conference on Advanced Materials*, Rio de Janeiro (Brasil) **2009**.
- [10] L. Song, S. Zhang, *Colloids and Surfaces A* **2009**, *348*, 217–2209.
- [11] L. Duan, S. Jia, Y. Wang, J. Chen, L. Zhao, *J. Mater. Sci.* **2009**, *44*, 4407–4412.
- [12] D. Todor, *Minerals thermal analysis*, Ed. Technic, Bucharest, **1972**.
- [13] D. Taloi, *Technological process optimisation. Applications in metallurgy*, Academy Ed. R.S.R., Bucharest, **1987**.